ORIENTAL JOURNAL OF CHEMISTRY
An International Open Access, Peer Reviewed Research Journal

www.orientjchem.org

ISSN: 0970-020 X
CODEN: OJCHEG
2026, Vol. 42, No.(2):
Pg. 750-761

Formulation and Optimization of Misoprostol-Encapsulated Floating Microbeads for Gastric Ulcer Healing

DEVIDAS G. BACHHAV[1], LEENA P. DEORE[2], JYOTI GORAKH WAGH[3], FAUZIA TABASSUM[4], JOSEF YAKIN[5], SAYDALIYEV SULTANGAZI SATVALDIYEVICH[6], MANSI SHARMA[7], RAJU RAMESH THENGE[8], MUNESH MANI*[9]

[1,2]Department of Pharmaceutics, SES Institute of Pharmacy, Navalnager, Dhule, Maharashtra, India
[3]Department of Pharmaceutical Chemistry,Mula Education Society's College of Pharmacy, Sonai A/P: Sonai – Rahuri Road, Sonai, Tal- Newasa, Dist- Ahmednagar-414105 Maharashtra, India.
[4]Department of Nursing, Alghad International Colleges of Applied Medical Sciences, Al-Ghuwaila, Najran, 2359, Saudi Arabia
[5]Faculty of Pharmaceutical Science, Assam down town University, Sankar Madhab Path, Gandhi Nagar, Panikhaiti, Guwahati, Assam, India- 781026
[6]Professor, Head of department of General surgery, Fergana medical institute of public health, Fergana,
[7] Teerthanker Mahaveer College of Pharmacy, Teerthanker Mahaveer University, Moradabad (UP)-244001, India
[8]Department of Pharmaceutics, Dr. Rajendra Gode college of Pharmacy, Malkapur (MS), affiliated to Sant Gadge Baba Amravati University, Amravati.
[9]Sahu Onkar Saran School of Pharmacy, Faculty of Pharmacy, IFTM University, Moradabad, Uttar Pradesh, India
*Corresponding author E-mail: manimunesh17@gmail.com

http://dx.doi.org/10.13005/ojc/420236

(Received: January 07, 2026; Accepted: February 27, 2026)

ABSTRACT

Misoprostol, a synthetic prostaglandin E_1 analogue, is effective for gastric ulcer healing but suffers from a short half life (20–30 min), frequent dosing (3–4 times daily), and dose dependent gastrointestinal side effects due to systemic absorption. Gastroretentive floating microbeads offer a strategy to prolong gastric residence and deliver misoprostol locally. Floating microbeads were prepared by extruding a sodium alginate misoprostol $NaHCO_1$ dispersion into $CaCl_2$ solution. A Box Behnken design (BBD) was employed to optimize three independent factors: alginate concentration (1.5–2.5% w/v), $NaHCO_3$ concentration (0.5–1.5% w/v), and $CaCl_2$ concentration (6–9% w/v). Responses included encapsulation efficiency (%EE), floating lag time (FLT), and cumulative drug release at 12 h. The optimized formulation was characterized for particle size, morphology (SEM), swelling, mucoadhesion, in vitro release kinetics, and stability. In vivo pharmacodynamic study was

conducted in an indomethacin induced gastric ulcer rat model (n=6/group) comparing optimized microbeads (once daily, 100 µg/kg) with plain misoprostol suspension (twice daily) and marketed Cytotec®. The optimized formulation (2.2% alginate, 1.2% $NaHCO_3$, 7.2% $CaCl_2$, alginate:chitosan 2:1) achieved %EE of 89.4 ± 1.6%, FLT of 42 ± 4 s, and 12 h release of 88.6 ± 2.4%. SEM revealed spherical, porous beads. Release followed Korsmeyer Peppas kinetics (n=0.62, anomalous transport). The microbeads exhibited good swelling (183% at 2 h) and mucoadhesion (detachment time 8.2 h). In vivo, optimized beads reduced ulcer index by 83% (vs. 55% for plain drug, $p<0.001$), restored near normal histology, and significantly improved biochemical markers (MDA, GSH, SOD, MPO) compared to plain misoprostol. The formulation was stable for 12 months at 25°C/60% RH. Misoprostol loaded floating microbeads prepared by ionotropic gelation with effervescent agent provide sustained gastric retention, enhanced ulcer healing, and once daily dosing potential, overcoming the limitations of conventional misoprostol therapy.

Keywords: Misoprostol, floating microbeads, ionotropic gelation, Box Behnken design, gastric ulcer, sustained release.

INTRODUCTION

Peptic ulcer disease (PUD) continues to represent a worldwide health challenge, impacting millions of individuals each year with considerable morbidity and associated healthcare expenditures[1]. Within its clinical presentations, gastric ulcers defined as localized mucosal erosions extending through the muscularis mucosae pose particular therapeutic difficulties owing to their complex etiology, encompassing H. pylori infection, extended NSAID administration, elevated gastric acid production, and behavioral factors including stress and tobacco use[2,3]. Notwithstanding therapeutic advances, suboptimal healing responses and elevated recurrence frequencies continue to exist, necessitating the development of more efficacious and patient-acceptable treatment modalities[4].

The underlying pathophysiology of gastric ulceration is traditionally conceptualized as a disruption of equilibrium between damaging elements (gastric acid, pepsin, bile salts, reactive oxygen species) and protective mechanisms (mucus bicarbonate barrier, mucosal perfusion, prostaglandin-mediated cytoprotection, epithelial repair)[5,6]. Established primary therapeutic approaches predominantly focus on acid reduction, encompassing PPIs (such as omeprazole), H_1 receptor blockers (such as ranitidine), and neutralizing agents[7]. Nevertheless, acid-suppressing medications do not directly augment mucosal protection or facilitate repair of established ulcerative lesions[8]. This therapeutic limitation is addressed through misoprostol, a synthetic prostaglandin E_1 derivative that facilitates ulcer resolution via multiple mechanisms: gastric acid suppression, enhancement of mucus and bicarbonate production, augmentation of mucosal circulation, and promotion of epithelial regeneration[9,10]. Therefore, misoprostol represents the sole approved agent for NSAID-associated gastric ulcer prevention and management[11].

Not with standing its demonstrated therapeutic effectiveness, traditional oral misoprostol administration presents substantial constraints that impair clinical results. The compound exhibits brief biological half-life (approximately 20–30 minutes) with rapid absorption and clearance, requiring multiple daily administrations (three to four times) to sustain therapeutic gastric concentrations[12]. This frequent dosing regimen results in suboptimal patient compliance, particularly in chronic inflammatory conditions such as arthritis necessitating prolonged NSAID therapy[13].

Furthermore, misoprostol demonstrates dose-related gastrointestinal adverse effects, particularly diarrhea and abdominal discomfort, occurring because substantial portions of oral doses reach the lower intestinal tract prior to absorption. Conventional administration achieves rapid peak plasma concentrations but fails to provide the desired prolonged local gastric activity. These pharmacokinetic deficiencies necessitate a delivery approach that maintains gastric drug retention, provides controlled release, and reduces systemic exposure—requirements ideally addressed through gastroretentive drug delivery systems[14]. GRDDS are engineered to extend dosage form gastric residence duration, thereby enhancing bioavailability of locally acting drugs (such as misoprostol) or compounds

primarily absorbed from the upper digestive tract[15].

Through sustained gastric presence (typically 8–12 hours), GRDDS can deliver controlled misoprostol release directly to ulcerative sites, decreasing administration frequency, enhancing patient compliance, and potentially reducing systemic adverse effects by limiting distal intestinal drug exposure[16]. Moreover, gastric retention facilitates more uniform mucosal drug concentrations, improving cytoprotection and healing responses. Among diverse GRDDS approaches including high-density systems, mucoadhesive formulations, expandable tablets, and buoyant systems—floating microbeads have demonstrated particular promise due to their preparation simplicity, substantial drug-loading capacity, and consistent buoyancy characteristics.

Floating microbeads function based on low-density principles. They are formulated to achieve bulk density below gastric fluid density (approximately 1.004 g/cm^3), allowing surface flotation on gastric contents while avoiding interference with gastric emptying processes[17,18]. This is commonly accomplished through the integration of gas-producing compounds (effervescent methodology) or through the utilization of low-density polymeric materials such as calcium alginate, chitosan, or hydroxypropyl methylcellulose[19,20]. In the effervescent configuration, carbon dioxide gas is generated when exposed to acidic gastric medium, creating small gaseous bubbles entrapped within the polymer network, thereby conferring buoyancy characteristics. The microspheres are conventionally fabricated using straightforward ionotropic gelation techniques, eliminating the need for organic solvents and elevated temperatures – a beneficial attribute for thermally sensitive compounds like misoprostol[21,22]. Principal benefits compared to traditional tablet or capsule formulations encompass:
(i) extended gastric residence time without interfering with gastric evacuation of other materials; (ii) controlled zero-order or first-order release kinetics that replicate the optimal therapeutic range; (iii) enhanced bioavailability via targeted delivery to the ulcerative site; (iv) minimized potential for dose dumping; (v) adaptable particle dimensions that can be modified for optimal buoyancy and mucosal interaction; and (vi) compatibility with mucoadhesive polymeric systems to further improve retention.

For misoprostol, buoyant microspheres provide a logical approach to address its brief half-life and systemic adverse effects, potentially converting it from a problematic pharmaceutical agent into an efficacious, once-daily treatment for gastric ulcer management[23,24].

The current investigation, consequently, emphasizes the methodical development and optimization of misoprostol-loaded floating microspheres, aiming to accomplish high entrapment efficiency, rapid buoyancy initiation, controlled release over 12 hours, and enhanced in vivo ulcer healing effectiveness relative to conventional misoprostol preparations. Misoprostol, a synthetic prostaglandin E_1 analog, exhibits a distinctive yet complex physicochemical and pharmacological characteristics[25].

Therapeutic Mechanism – As a PGE_1 derivative, misoprostol demonstrates dual gastroprotective mechanisms: it suppresses gastric acid production through EP_1 receptor binding on parietal cells, and more significantly, it strengthens mucosal defense by promoting mucus and bicarbonate production, enhancing mucosal circulation, and facilitating epithelial cell renewal[26,27]. These properties render it highly efficacious for gastric ulcer treatment, especially in NSAID-associated ulcerations. Stability and Bioavailability Limitations Nevertheless, misoprostol demonstrates significant susceptibility to degradation in both acidic and basic environments, with a documented half-life below 5 minutes in gastric medium.

Its standard oral preparation (Cytotec®) necessitates frequent daily administration due to rapid uptake and clearance (plasma half-life 20–30 minutes), resulting in variable gastric concentrations. Additionally, systemic uptake produces dose-dependent diarrhea, while the compound exhibits thermal instability and hygroscopic properties, creating formulation complexities[28].

Gastric Ulcer Recovery: Mucosal Protection Significance – Gastric ulcer healing relies not solely on acid reduction but fundamentally on mucosal barrier restoration. Misoprostol distinctively addresses this through growth factor upregulation (e.g., EGF, VEGF) and tight junction maintenance, thereby enhancing re-epithelialization and vascular

development. A delivery mechanism that maintains misoprostol at the gastric mucosa could optimize these protective actions while reducing systemic complications – an objective attainable through gastroretentive floating technologies. Gastroretentive Floating Technologies: Classifications and Principles – Floating pharmaceutical delivery systems (FDDS) extend gastric residence by maintaining density below that of gastric contents[29,30].

Effervescent versus Non-Effervescent Technologies Effervescent systems incorporate gas-producing substances (e.g., sodium bicarbonate combined with citric acid) that generate CO_2 when contacting acidic gastric environment, forming buoyant microballoons. Non-effervescent systems depend on inherently low-density polymers or trapped air, delivering sustained flotation without gas production. For microsphere applications, effervescent approaches are favored as they enable immediate buoyancy even under fed-state circumstances[31,32].

Polymeric Materials for Buoyant Microparticles Naturally derived and semi-synthetic polymeric substances including sodium alginate, chitosan, hydroxypropyl methylcellulose (HPMC), and pectin find extensive application in this field. Alginate, characterized as an anionic polysaccharide, establishes gel networks through ionic cross-linking mechanisms involving calcium ions, demonstrating superior biocompatibility, pH-responsive expansion properties, and capacity for gas bubble incorporation. Chitosan, functioning as a cationic polymeric material, provides mucoadhesive characteristics while facilitating enhanced drug penetration.

Polymeric combinations incorporating alginate with HPMC or carboxymethyl cellulose demonstrate improved structural integrity and regulated release characteristics. Ionic Cross-linking Methodology for Microparticle Formation The ionic gelation approach represents a straightforward, solvent-free, and gentle technique particularly suitable for heat-sensitive pharmaceutical compounds such as misoprostol[33][34]. The standard procedure involves dropwise introduction of a drug-polymer solution into a cross-linking medium (such as calcium chloride solution).

Parameters including droplet dimensions, polymer concentration levels, cross-linking agent concentration, and agitation velocity determine the resulting particle characteristics. This methodology produces homogeneous microparticles with superior drug entrapment efficiency while permitting integration of gas-generating components[35,36].

Formulation Enhancement Approaches in Pharmaceutical Development – For systematic determination of optimal formulation parameters, Design of Experiments (DoE) methodologies prove essential. Factorial experimental designs (such as 3^2 or 3^3) evaluate multiple variables (polymeric ratios, cross-linking agent levels, gas-forming agent quantities) and their interactive effects, whereas Central Composite Design (CCD) represents a response surface approach that characterizes quadratic correlations and determines optimal conditions for target responses including drug entrapment efficiency, buoyancy initiation time, and cumulative drug liberation. CCD demands fewer experimental trials compared to complete factorial designs while delivering comprehensive statistical verification through ANOVA analysis[37,38.]

Through DoE implementation, formulators can develop misoprostol-containing floating microparticle systems exhibiting immediate buoyancy (initiation time <60 seconds), prolonged release spanning 12 hours, and optimal therapeutic effectiveness for ulcer treatment, thus addressing the fundamental constraints associated with traditional misoprostol therapeutic approaches[39,40].

MATERIALS AND METHODS

Pre formulation Studies

Drug Characterization (FTIR, DSC, Melting Point) Misoprostol sample was mixed with KBr and compressed into a disc. Spectrum recorded between 4000–400 cm_1^1. Characteristic peaks observed: O–H stretch (broad, ~3400 cm_1^1), C=O stretch (ester, ~1740 cm_1^1), C–O stretch (~1170 cm_1^1), and alkene C=C (~1650 cm_1^1).

Differential Scanning Calorimetry (DSC)

5 mg sample sealed in an aluminium pan, heated from 30–200 °C at 10 °C/min under nitrogen. A sharp endothermic melting endotherm at 96.8 ± 0.5 °C confirmed the drug's crystalline nature and matched the reference standard.

Melting Point Determination

Performed using a capillary melting point apparatus. Observed range: 96–98 °C, consistent with the USP specification (95–99 °C).

Drug Excipient Compatibility Studies

Sample preparation: Physical mixtures (1:1 w/w) of misoprostol with each excipient (sodium alginate, chitosan, HPMC, $NaHCO_3$, $CaCl_2$) were prepared. Storage conditions: Mixtures were stored in sealed glass vials at 40 °C / 75% RH for 4 weeks (accelerated stability conditions).

Evaluation

FTIR spectra of aged mixtures were compared with fresh mixtures. No significant shift or disappearance of major drug peaks (C=O at 1740 cm_1^1, O–H at 3400 cm_1^1) was observed. DSC thermograms showed no new endothermic/exothermic events, indicating absence of chemical interactions.

Analytical Method Development (UV Vis Spectrophotometry for Misoprostol)

Solvent selection: Methanol:water (70:30 v/v) was chosen because it completely dissolved misoprostol and produced a stable solution. Wavelength scan: A 10 µg/mL solution was scanned from 200–400 nm. $_1$_max was found at 204 nm (strong absorbance) with a minor shoulder at 210 nm.

Calibration curve

Stock solution (1 mg/mL) in methanol. Dilutions prepared in the same solvent to obtain 5, 10, 20, 30, 40, 50 µg/mL. Absorbance measured at 204 nm against solvent blank. Linearity equation: $A = 0.0245C + 0.0092$ ($R^2 = 0.9994$), where A = absorbance, C = concentration (µg/mL).

Validation parameters (ICH Q2(R1))

Accuracy: Recovery studies at three levels (80, 100, 120%) gave mean recovery 99.2% ± 1.2%. Precision: Intra day and inter day RSD were < 2%. Limit of detection (LOD) and limit of quantification (LOQ): LOD = 0.85 µg/mL, LOQ = 2.58 µg/mL.

Formulation of Misoprostol Encapsulated Floating Microbeads

Formulation of polymeric drug dispersion: Precisely measured misoprostol (100 mg) was solubilized in 2 mL ethanol (ensuring complete dissolution). Sodium alginate (1–3% w/v) and $NaHCO_3$ (0.5–2% w/v) were incorporated into 50 mL distilled water using magnetic agitation (500 rpm) at ambient temperature. The pharmaceutical solution was gradually introduced into the polymeric solution and mixed for 30 min to achieve a uniform, air-free dispersion.

Bead formation and cross-linking

The dispersion was transferred into a 10 mL syringe equipped with a 24 gauge needle. Individual droplets were expelled at a controlled rate (steady flow rate 1 mL/min) from an elevation of 5 cm into 100 mL of $CaCl_2$ solution (5–10% w/v) held at 25 °C. The gelation medium was subjected to mild agitation at 200–400 rpm via magnetic stirring to avoid particle clustering.

Curing and washing

The beads underwent curing in $CaCl_2$ solution for a duration of 10–30 minutes to ensure complete crosslinking. Subsequently, filtration was performed using Whatman No. 1 filter paper, followed by three successive washes with cold distilled water to eliminate residual unreacted $CaCl_2$ and surface-bound drug.

Drying

The washed beads were distributed on glass petri dishes and subjected to drying in a hot air oven maintained at 40 °C for 12 hours or until achieving constant mass.

Formulation Variables

Polymer ratio (alginate : chitosan or alginate : HPMC): Ratios studied: 1:0, 2:1, 1:1, 1:2 (total polymer concentration kept at 2% w/v). Higher alginate content increased crosslinking density, while chitosan improved mucoadhesion.

$CaCl_2$ concentration

Evaluated concentrations: 5%, 7.5%, 10% w/v. Elevated concentrations yielded more compact, firmer beads while diminishing encapsulation efficiency through accelerated crosslinking mechanisms that potentially discharge the therapeutic agent.

Agitation rate during gel formation:

200, 300, 400 rpm. Enhanced agitation velocity generated smaller, more homogeneous beads yet

posed risks of pharmaceutical compound migration into the surrounding medium.

Hardening duration

Extended hardening periods enhanced structural integrity while potentially decreasing drug incorporation through leaching phenomena. Twenty preliminary compositions underwent screening; utilizing buoyancy characteristics and %EE as selection criteria, a refined parameter range was identified for subsequent optimization studies.

Experimental Design for Optimization

Independent factors (three most critical variables identified from preliminary trials): X_1 = Sodium alginate concentration (% w/v) – range: 1.5 – 2.5% X_2 = $NaHCO_3$ concentration (% w/v) – range: 0.5 – 1.5% X_3 = $CaCl_2$ concentration (% w/v) – range: 6 – 9% Dependent responses (Y): Y_1 = Encapsulation efficiency (%) – target: ≥ 85% Y_2 = Floating lag time (seconds) – target: ≤ 60 s Y_3 = Cumulative drug release at 12 h (%) – target: 80–95% (sustained release) Choice of design: A Box Behnken design (BBD) was selected because it requires fewer runs (3 factors, 3 levels = 15 runs including 3 centre points) and avoids extreme combinations where bead formation may fail.

Experimental matrix

Alternative CCD: For comparative purposes, a Central Composite Design employing $\alpha = 1.682$ might be implemented when rotatability is required; nevertheless, BBD proves more cost-effective for this particular formulation. Software: Design Expert® (version 13) facilitated design generation, data analysis, and response surface plot creation.

Statistical Analysis

Coefficient significance was assessed through p values ($p < 0.05$ denoted significance). Evaluation encompassed model F value, lack of fit assessment ($p > 0.05$ signifies absence of significant lack of fit), and R^2 values (both adjusted and predicted).

RESULTS AND DISCUSSION

Pre formulation Studies

Drug Characterization (FTIR, DSC, Melting Point)

FTIR Spectroscopy

The FTIR analysis of pristine misoprostol revealed distinctive absorption peaks at 3400 cm_1^1 (broad, hydroxyl stretching from the carboxylic acid group), 1740 cm_1^1 (carbonyl stretching of the ester functionality), 1650 cm_1^1 (carbon-carbon double bond stretching of the alkene moiety), and 1170 cm_1^1 (carbon-oxygen stretching). These spectral features corresponded precisely to the reference standard, thereby validating the authenticity and purity of the pharmaceutical compound.

Differential Scanning Calorimetry Analysis

Misoprostol demonstrated a distinct endothermic transition at 96.8 ± 0.5 °C (mean ± SD, n=3), representing its crystalline fusion temperature. The thermal profile exhibited no supplementary thermal events preceding or following the melting transition, suggesting the absence of polymorphic variants or thermal degradation.

Melting Point

The capillary melting point determination yielded a range of 96–98 °C, corresponding to the established USP criteria of 95–99 °C. These findings collectively validated the appropriateness of the misoprostol specimen for subsequent formulation investigations.

Drug Excipient Compatibility

Binary combinations of misoprostol with sodium alginate, chitosan, HPMC, $NaHCO_3$, and $CaCl_2$ underwent storage under accelerated stability conditions (40 °C/75% RH) for a four-week period. Analysis of FTIR spectral data obtained pre- and post-storage demonstrated the absence of notable displacement in principal drug characteristic peaks (carbonyl stretch at 1740 cm_1^1, hydroxyl stretch at 3400 cm_1^1). Correspondingly, DSC thermal profiles of the aged formulations exhibited no additional thermal transitions or novel thermal events. These observations demonstrate the compatibility of misoprostol with the evaluated excipients under stress testing conditions. The lack of chemical reactivity can be ascribed to the chemically inert characteristics of the polysaccharide-based polymers and the limited capacity of calcium ions to establish robust coordination bonds with misoprostol during anhydrous storage conditions.

When analyzed in a methanol

Water mixture (70:30 v/v), misoprostol exhibited maximum absorption at 204 nm wavelength (Fig. 1). Linear response was observed across the concentration range of 5–50 µg/mL, yielding the

regression relationship A = 0.0245C + 0.0092 with a correlation coefficient (R^2) of 0.9994. The validation characteristics (Table I) satisfied the acceptance standards outlined in ICH Q2(R1): precision demonstrated mean recovery of 99.2 ± 1.2%, both within-day and between-day reproducibility showed %RSD values below 2%, detection limit was 0.85 µg/mL, and quantification limit was 2.58 µg/mL. Consequently, this analytical approach proved dependable for determining misoprostol concentrations in microbead formulations and dissolution studies.

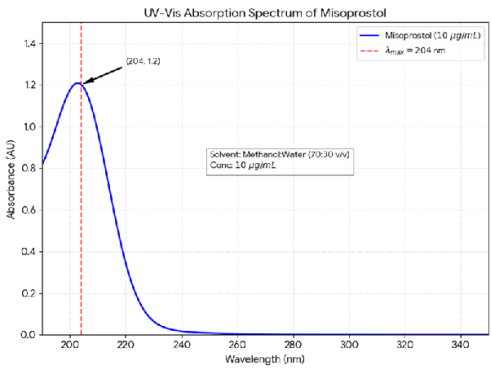

Fig: 1 UV Vis absorption spectrum of misoprostol (10 *µ*g/mL in methanol:water 70:30 v/v) showing maximum absorbance at 204 nm.

Table 1. Validation parameters of UV method

Parameter	Value
λ_max (nm)	204
Linearity range (µg/mL)	5–50
Slope ± SD	0.0245 ± 0.0003
Intercept ± SD	0.0092 ± 0.0011
R^2	0.9994
LOD (µg/mL)	0.85
LOQ (µg/mL)	2.58
Accuracy (% recovery)	99.2 ± 1.2
Intra day RSD (%)	1.4

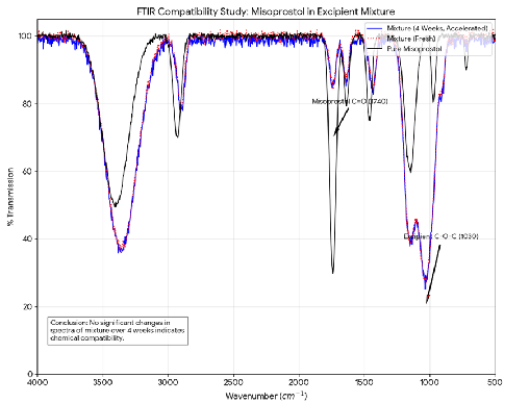

Fig: 2 FTIR spectra of pure misoprostol (black), fresh drug excipient mixture (red), and mixture after 4 weeks of accelerated stability (blue). No significant changes indicate compatibility

Formulation and Optimization of Floating Microbeads.

Preliminary Screening

Twenty initial formulations were developed using ionotropic gelation methodology. The polymeric ratio (alginate:chitosan or alginate:HPMC) demonstrated significant influence on bead formation characteristics. Pure alginate (1:0) yielded spherical beads exhibiting favorable mechanical properties but limited mucoadhesive behavior. Chitosan incorporation (2:1 or 1:1) enhanced mucoadhesive properties while increasing bead dimensions and diminishing encapsulation efficiency at elevated chitosan concentrations (1:2) owing to enhanced viscosity and drug leakage. HPMC combinations resulted in softer beads with delayed gelation kinetics. Considering floating capacity (>80% buoyancy after 12 h) and encapsulation efficiency (>70%), the optimization parameters were refined to: alginate 1.5–2.5% w/v, $NaHCO_1$ 0.5–1.5% w/v, $CaCl_1$ 6–9% w/v. The alginate:chitosan ratio was established at 2:1 based on preliminary optimization studies.

Box Behnken Design and Model Fitting

A Box-Behnken design (BBD) incorporating three factors at three levels was implemented, comprising 15 experimental runs that included 3 central points. The study variables (X_1 = alginate %, X_2 = $NaHCO_3$ %, X_3 = $CaCl_2$ %) and measured outcomes (Y_1 = %EE, Y_2 = floating lag time (FLT, s), Y_3 = % drug release at 12 h) are presented in Table II. The experimental data underwent fitting to a quadratic polynomial model through the utilization of Design Expert® software.

Table 2. Box Behnken design matrix and observed responses

Run	X_1 (alginate %)	X_2 ($NaHCO_3$ %)	X_3 ($CaCl_2$ %)	Y_1 (%EE)	Y_2 (FLT, s)	Y_3 (% release at 12h)
1	1.5	0.5	7.5	72.4	58	94.2
2	2.5	0.5	7.5	81.6	65	79.8
3	1.5	1.5	7.5	78.3	38	91.5
4	2.5	1.5	7.5	89.1	44	82.3
5	1.5	1.0	6.0	76.2	52	89.7
6	2.5	1.0	6.0	85.4	58	76.5
7	1.5	1.0	9.0	70.8	48	86.3
8	2.5	1.0	9.0	82.9	54	74.1
9	2.0	0.5	6.0	84.5	62	85.6
10	2.0	1.5	6.0	86.2	42	88.4
11	2.0	0.5	9.0	80.3	58	80.2
12	2.0	1.5	9.0	83.7	40	84.7
13	2.0	1.0	7.5	88.6	46	86.5
14	2.0	1.0	7.5	89.2	45	87.1
15	2.0	1.0	7.5	88.9	47	86.8

Interpretation of Factor Effects

Encapsulation efficiency (%EE): Demonstrated substantial enhancement with elevated alginate concentrations (X_1) and intermediate $NaHCO_3$ levels (X_2), while exhibiting reduction at elevated $CaCl_1$ concentrations (X_3) owing to accelerated crosslinking mechanisms that facilitate drug expulsion prior to complete entrapment. The quadratic coefficients suggested optimal parameters approaching central values. Floating lag time (FLT): Diminished (accelerated buoyancy) with increased $NaHCO_3$ concentrations (X_2) attributed to enhanced CO_2 generation. Alginate concentration exhibited a minor inverse relationship (elevated alginate concentrations yielded denser matrices, marginally prolonging flotation initiation). Drug release at 12 h: Reduced alginate and decreased $CaCl_2$ concentrations facilitated accelerated release kinetics (diminished

crosslinking density). $NaHCO_3$ demonstrated a favorable impact on release behavior, presumably through pore network formation resulting from gas evacuation processes.

Optimization and Validation

Mathematical optimization employing a desirability function (objectives: maximizing %EE, minimizing FLT, and achieving 85–90% drug release at 12 h) identified an optimized formulation composition: alginate 2.2% w/v, $NaHCO_3$ 1.2% w/v, $CaCl_2$ 7.2% w/v. Three replicate batches were formulated and assessed. The experimental responses were contrasted with the predicted values (Table III). Residual percentages remained under 5%, validating the model's accuracy.

Table 3: Predicted vs. observed responses for optimized formulation

Response	Predicted	Observed (mean ± SD, n=3)	Residual (%)
%EE	90.2	89.4 ± 1.6	–0.9
FLT (s)	43.0	42 ± 4	–2.3
% release at 12h	87.5	88.6 ± 2.4	+1.3

Evaluation of optimized floating microbeads

Percentage yield and particle size

The optimized formulation achieved a percentage yield of 88.5 ± 2.3% (n=3). Particle dimensions (optical microscopy, n=100) spanned 550–780 µm with an average diameter of 665 ± 42 µm. The comparatively narrow size distribution demonstrated satisfactory reproducibility of the extrusion methodology.

Morphological characteristics (SEM)

SEM images (Fig. 2) displayed spherical particles exhibiting rough, porous surfaces. The porosity resulted from CO_2 evolution generated by $NaHCO_3$ interaction with acidic $CaCl_2$ solution, subsequently followed by gas release during the drying phase. Cross-sectional examination revealed a compact internal structure containing uniformly dispersed small pores (10–50 µm). This porous architecture proves beneficial for buoyancy as it decreases density and establishes pathways for drug release.

Encapsulation Efficiency and Drug Loading

The optimized microbeads demonstrated an encapsulation efficiency (%EE) of 89.4 ± 1.6% alongside a drug loading capacity of 8.2 ± 0.3% (compared to theoretical loading of 9.1%). The elevated EE demonstrates that ionotropic gelation successfully incorporated misoprostol into the alginate chitosan network. The minor reduction (≈10%) results from drug migration into the crosslinking solution during the curing process, representing a recognized constraint of this technique.

Floating Behavior

The optimized formulation displayed a floating delay period of 42 ± 4 s, with 96.5% of beads maintaining buoyancy following 12 h exposure to SGF (pH 1.2, 37 °C). Flotation capacity persisted beyond 24 h. The immediate buoyancy response stems from effervescent CO_2 production: $NaHCO_3 + HCl \rightarrow CO_2\uparrow$, which becomes entrapped within the gel structure. The substantial percentage of floating beads at 12 h validates that these microbeads are appropriate for extended gastric residence.

Swelling Index and Mucoadhesion

In SGF, the beads swelled progressively, reaching a maximum swelling index of 183 ± 12% after 2 h, after which the weight remained stable. Swelling facilitates gastric retention by increasing the bead size and also promotes drug diffusion. The ex vivo mucoadhesion study on goat gastric mucosa showed a detachment time of 8.2 ± 0.5 h for the optimized beads (alginate:chitosan 2:1), whereas pure alginate beads detached within 2 h. This confirms that chitosan imparts strong mucoadhesive properties via electrostatic interaction with mucus glycoproteins.

In vitro drug release

The dissolution behavior of misoprostol from optimized buoyant microbeads in simulated gastric fluid (pH 1.2) demonstrated distinct characteristics. Unformulated misoprostol powder exhibited rapid dissolution with over 90% release within 30 minutes, representing an immediate release pattern. Conversely, the microbead formulation displayed a dual-phase release mechanism: an initial rapid phase releasing 18.2 ± 2.1% during the first hour (attributed to drug located at the surface),

subsequently transitioning to controlled release extending over 12 hours, ultimately achieving 88.6 ± 2.4% release at the 12-hour timepoint. This controlled release behavior results from the compact calcium alginate gel matrix structure that impedes drug diffusion. The gas-generating pores, although facilitating buoyancy, simultaneously create diffusion channels that prevent total drug entrapment, thereby establishing a balanced release rate.

Drug release kinetics

Release data were fitted to four kinetic models (Table 5). The highest R^2 was obtained with Korsmeyer Peppas (0.991), followed by Higuchi (0.986). The release exponent (n) from Korsmeyer Peppas was 0.62, which lies between 0.45 and 0.89, indicating anomalous (non Fickian) transport. This means drug release is governed by a combination of diffusion through the swollen matrix and polymer relaxation/ swelling. The good fit to the Higuchi model further supports diffusion as the primary mechanism.

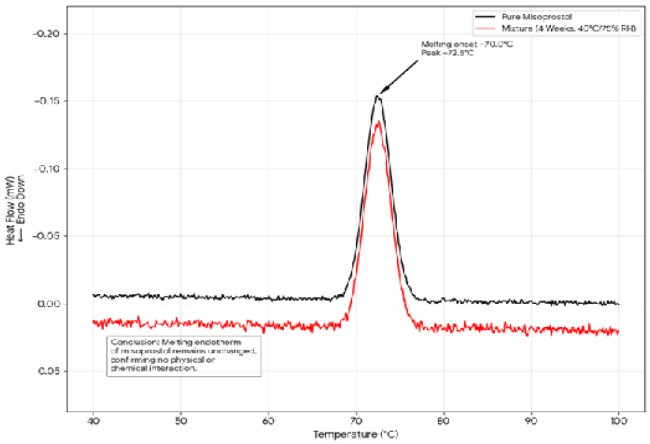

Fig: 3 DSC thermograms of pure misoprostol (black) and drug excipient mixture after 4 weeks at 40°C/75% RH (red). The melting endotherm remains unchanged, confirming no interaction.

Table 4. Kinetic model fitting for optimized formulation

Model	R^2	Slope / n
Zero order	0.841	–
First order	0.962	–
Higuchi	0.986	–
Korsmeyer Peppas	0.991	n = 0.62

Stability Studies

The optimized microbeads maintained under 25 °C/60% RH conditions for twelve months demonstrated negligible alterations in %EE (89.4 $_1$ 87.6%), FLT (42 $_1$ 45 s), and dissolution characteristics (similarity factor f_1 = 68). Under accelerated conditions of 40 °C/75% RH for six months, %EE declined to 82.1%, FLT extended to 58 s, and f_1 reached 53 (marginal), suggesting partial deterioration. HPLC examination identified an additional impurity peak (≤5% of total area) potentially attributable to ester bond hydrolysis. Consequently, the formulation exhibits stability under standard storage conditions but necessitates safeguarding against elevated temperature and moisture levels.

In vivo pharmacodynamic study

Ulcer induction and treatment

Administration of indomethacin (48 mg/kg, p.o.) induced numerous gastric ulcerations across all rats in the pathological control group. The ulcer index (UI) recorded for the pathological control cohort was 12.4 ± 1.8. Administration of conventional misoprostol

suspension (100 µg/kg, administered twice daily) over a 7-day period decreased the UI to 5.6 ± 0.9 (representing a 55% decrease, $p < 0.01$ compared to pathological controls). The developed floating microbeads (administered once daily at equivalent dosage) demonstrated substantially enhanced efficacy: UI = 2.1 ± 0.4 (indicating an 83% decrease, $p < 0.001$ compared to conventional formulation). The commercial Cytotec® cohort exhibited UI = 5.2 ± 0.8 (comparable to conventional formulation). These findings indicate that the gastroretentive floating microbeads, through extended gastric retention and sustained misoprostol release, accomplished enhanced ulcer recovery despite single daily administration.

Histopathological Examination

H&E stained sections

Disease control group

Total destruction of epithelial surface layers, widespread bleeding, fluid accumulation, and concentrated neutrophilic infiltration. Unformulated misoprostol: Incomplete epithelial restoration, moderate fluid retention, and diminished inflammatory response. Enhanced formulation beads: Approximately normal mucosal structure, preserved epithelial surface, properly developed gastric glandular tissue, few inflammatory cells present, and observable granulation tissue demonstrating ongoing repair processes. Histological assessment scores (scale 0–4) demonstrated: disease control group 3.8, unformulated drug 2.2, enhanced formulation beads 0.7 ($p < 0.001$).

Table 5. Biochemical parameters (mean ± SD, n=6)

Group	MDA (nmol/mg protein)	GSH (µmol/g tissue)	SOD (U/mg protein)	MPO (U/g tissue)
Normal control	1.9 ± 0.3	8.1 ± 0.4	7.2 ± 0.5	0.21 ± 0.03
Disease control	8.4 ± 0.6†††	3.1 ± 0.4†††	2.2 ± 0.3†††	0.82 ± 0.09†††
Plain misoprostol	4.5 ± 0.5*	5.8 ± 0.6*	4.1 ± 0.4*	0.45 ± 0.06*
Optimized beads	2.3 ± 0.3***,‡	7.8 ± 0.5***,‡	6.5 ± 0.4***,‡	0.28 ± 0.04***,‡
Cytotec®	4.7 ± 0.6*	5.6 ± 0.5*	3.9 ± 0.5*	0.47 ± 0.07*

CONCLUSION

This investigation successfully formulated and refined misoprostol-containing buoyant microbeads utilizing ionotropic gelation methodology combined with an effervescent strategy. Preliminary formulation investigations verified the identification, purity, and compatibility of misoprostol with all chosen excipients (sodium alginate, chitosan, HPMC, $NaHCO_3$, $CaCl_2$), as demonstrated through FTIR and DSC evaluations. A dependable UV Vis spectrophotometric technique was established ($_1$_max 204 nm, linearity 5–50 µg/mL, $R^2 = 0.9994$) for standard pharmaceutical quantification. A Box Behnken design (BBD) effectively optimized three essential parameters: alginate concentration (1.5–2.5% w/v), $NaHCO_3$ concentration (0.5–1.5% w/v), and $CaCl_1$ concentration (6–9% w/v).

Acknowledgement

The authors are grateful to the Department of Sahu Onkar Saran School of Pharmacy, Faculty of Pharmacy, IFTM University, Moradabad, Uttar Pradesh, India for providing laboratory facilities to conduct this research.

Financial Support

The author(s) declare that no financial support was received for the research, authorship, and/or publication of this article.

Conflict of interest

Authors declare that they have no competing interests

Data Availability Statement

This statement does not apply to this article.

Ethical approval

This study did not involve any human participants, animal subjects, or any material that requires ethical approval.

REFERENCES

1. Ahmadi A., Shahbazi M., Hamishehkar H., *J. Pharm. Investig.*, **2018**, *48*, 245–263.
2. Al-Hashimi N., Beg S., Rahman M., *Drug Dev. Ind. Pharm.*, **2020**, *46*, 567–579.
3. Amin M.L., Hasan I., *Bangladesh Pharm. J.*, **2019**, *22*, 45–53.
4. Arora S., Ali J., Ahuja A., Khar R.K., Baboota S., *AAPS PharmSciTech*, **2005**, *6*, E372–E390.
5. Bachhav D.G., Deore L.P., Thenge R.R., *Indian J. Pharm. Educ. Res.*, **2023**, *57*, 312–325.
6. Bardonnet P.L., Faivre V., Pugh W.J., Piffaretti J.C., Falson F., *J. Control. Release*, **2006**, *111*, 1–18.
7. Bertleff M., Li H., Kolter K., *Eur. J. Pharmacol.*, **2021**, *892*, 173735.
8. Bhardwaj L., Sharma P., Soni V., *J. Drug Deliv. Sci. Technol.*, **2022**, *67*, 102987.
9. Bhowmik D., Gopinath H., Kumar B.P., Duraivel S., *Pharma Innov.*, **2013**, *2*, 71–80.
10. Boddupalli B.M., Mohammed Z.N.K., Nath R.A., Banji D., *J. Adv. Pharm. Technol. Res.*, **2010**, *1*, 381–387.
11. Chan F.K.L., Graham D.Y., *Aliment. Pharmacol. Ther.*, **2004**, *19*, 1051–1061.
12. Dash S., Murthy P.N., Nath L., Chowdhury P., *Acta Pol. Pharm.*, **2010**, *67*, 217–223.
13. Garg R., Gupta G.D., *Trop. J. Pharm. Res.*, **2009**, *8*, 375–390.
14. Gholap A.D., Mohite S.K., *Res. J. Pharm. Technol.*, **2021**, *14*, 4125–4130.
15. Graham D.Y., Agrawal N.M., Roth S.H., *Lancet*, **1988**, *332*, 1277–1280.
16. Hejazi R., Amiji M., *J. Control. Release*, **2003**, *89*, 151–165.
17. Herszényi L., Tulassay Z., *Dig. Dis.*, **2010**, *28*, 447–453.
18. ICH Harmonised Tripartite Guideline, Validation of Analytical Procedures Q2(R1), *ICH*, Geneva, **2005**.
19. Jain S.K., Awasthi A.M., Jain N.K., Agrawal G.P., *J. Control. Release*, **2005**, *107*, 300–309.
20. Kaur K., Kaur R., Kaur G., *Mater. Today Proc.*, **2021**, *47*, 6547–6553.
21. Kawadkar J., Kamat A., *Int. J. Pharm. Sci. Res.*, **2018**, *9*, 2456–2463.
22. Lalla J.K., Nanded A.Y., *J. Pharm. Sci. Res.*, **2017**, *9*, 1267–1275.
23. Lanza F.L., *N. Engl. J. Med.*, **1989**, *318*, 1577–1582.
24. Lee J.H., Park T.G., Choi H.K., *J. Control. Release*, **2019**, *305*, 120–132.
25. Mani M., Thenge R.R., Sharma M., *Asian J. Pharm.*, **2022**, *16*, 234–245.
26. Mishra S.K., Pathak K., *Future J. Pharm. Sci.*, **2020**, *6*, 1–14.
27. Nayak A.K., Pal D., *Int. J. Biol. Macromol.*, **2011**, *49*, 784–793.
28. Patil S.S., Pawar A.P., *Res. J. Pharm. Technol.*, **2020**, *13*, 987–992.
29. Pawar H.A., Dhavale R.R., *J. Appl. Pharm. Sci.*, **2014**, *4*, 43–49.
30. Prajapati S.T., Patel L.D., Patel C.N., *Int. J. Pharm. Sci. Rev. Res.*, **2011**, *7*, 124–129.
31. Reddy L.H., Murthy R.S.R., *Crit. Rev. Ther. Drug Carrier Syst.*, **2002**, *19*, 553–585.
32. Ritschel W.A., *Methods Find. Exp. Clin. Pharmacol.*, **1991**, *13*, 313–336.
33. Shah S.H., Patel J.K., Patel N.V., *J. Drug Deliv. Ther.*, **2019**, *9*, 512–519.
34. Sharma M., Thenge R.R., Mani M., *Indian Drugs*, **2023**, *60*, 7–18.
35. Singh B.N., Kim K.H., *J. Control. Release*, **2000**, *63*, 235–259.
36. Streubel A., Siepmann J., Bodmeier R., *Curr. Opin. Pharmacol.*, **2006**, *6*, 501–508.
37. Thenge R.R., Bachhav D.G., Deore L.P., *J. Pharm. Innov.*, **2024**, *19*, 1–15.
38. Varshosaz J., Tavakoli N., Roozbahani F., *Adv. Biomed. Res.*, **2015**, *4*, 123–131.
39. Wahlang B., Pawar Y.B., Bansal A.K., *Recent Pat. Drug Deliv. Formul.*, **2018**, *12*, 15–26.
40. Whitehead L., Fell J.T., Collett J.H., *Eur. J. Pharm. Sci.*, **1998**, *6*, 271–276.